유공압건설기계학회논문집 제9권 제1호 pp. 10~17 2012년 3월

압력커플링 정유압 변속기를 이용한 에너지 절감 유압시스템에 관한 연구
A Study of Energy Saving Hydraulic System by A Pressure Coupling Hydrostatic Transmission

도황팅 · 안경관
H. T. Do and K. K. Ahn

접수일: 2011년 10월 29일, 수정일: 2012년 2월 24일, 게재확정일: 2012년 2월 25일

Key Words : Secondary Control(2차 제어), Pressure Coupling(압력 커플링), Braking Energy(제동에너지) Regeneration(재생), Hydrostatic Transmissions(정유압 변속기), Accumulator(어큐뮬레이터)

Abstract: Nowadays, the demand of energy saving is increasing more and more while the natural resources have been exhausted. Besides, the emission gas caused by vehicles has been being a serious environment problem. Therefore, many studies have been carried out, especially focusing on braking energy regeneration, in order to save energy as well as reduce emission of mobile vehicles. In this paper, we propose a closed-loop hydrostatic transmission for braking energy regeneration with two configurations to reduce the energy consumption by recovering the braking energy. The effectiveness of the proposed system was verified by simulation. The simulation results indicated that the pressure coupling configuration gave better performance in comparison to flow coupling configuration about 40.8%, 61.7% and 53.8% reduction of fuel consumption in 10 mode, 10 mode modified profile and highway schedules, respectively.

Nomenclature

$A_{r1,2}$: valve throttling area
C : viscous friction coefficient
C_d : discharge coefficient
D_{max} : max. Displacement of hydraulic machine
J : moment of inertia of flywheel
K_{sv} : DC gain of the mechanism
$E_{k,\max}$: max. Kinetic energy during deceleration
n : adiabatic coefficient
p_0 : pre-charged pressure
p_g : pressure of gas in accumulator
p_i : pressure at port of accumulator
$p_{pcv1,2}$: setting pressure of pilot check valve PCV1,2
p_r : return line pressure
p_s : driving/supply line pressure
Q_b : boost flow rate
Q_i: ideal flow rate of hydraulic machine
Q_{ha} : flow rate into accumulator
Q_l : loss flow rate of hydraulic machine
Q_{mi} : flow rate into the inlet port of the motor
Q_{mo} : flow rate from motor outlet port
Q_{pm} : actual flow rate of hydraulic machine
Q_{po} : output flow rate of the pump
$Q_{r1,2}$: flow rate via relief valve RV1,2
T_{ex} : external torque
T_l : loss torque of hydraulic machine
T_m : torque of hydraulic motor
$u(t)$: electric signal control
u_2 : displacement ratio of pump/motor PM2
V_0 : volume of hydraulic accumulator
V_f : fluid volume in the accumulator
V_h : volume of fluid in the hose
a : displacement ratio
Δp : pressure difference
τ : time constant of DCM
w : flywheel speed
δ : valve throttling area proportionality coefficient

안경관(주저자): 울산대학교 기계공학부
E-mail: kkahn@ulsan.ac.kr, Tel:052-259-2282
도황팅: 울산대학교 대학원 기계자동차공학과

Subscripts

u : upper
l : lower

1. Introduction

Reduction of energy consumption is one of the most important topics in vehicle research. Many researches about saving energy have been done. In hydraulic systems, hydrostatic transmissions(HST), constant pressure systems(CPS), electro-hydraulic actuators(EHA) and secondary control systems with common pressure rails(CPR) have been considered for energy-saving. In a HST system, the velocity of the motor is continuously controlled by adjusting the pump flow rate. Thus, it is suitable for earth moving machines such as wheel loaders, tractors and forklifts, etc[1]. However, the HST system cannot recover kinetic energy of the load, consequently, restricting its energy-saving potential. A CPS system employs a flywheel with an auxiliary hydraulic machine so that it is able to recover kinetic energy of the load and reuse recovered energy. The CPS system studies in 2) and 3) have shown that these systems are adequate for mobile applications, such as vehicles. However, the flywheel in CPS makes noise when operating and the kinetic energy of flywheel is gradually decreasing according to time. In an EHA system, batteries or super-capacitors are employed to store kinetic energy of the load[4),14),15),16)]. The EHA system has high recovery efficiency and good performance but its applicability is restricted due to its low specific power with batteries and high price with super-capacitors. In a CPR system, two common rails are employed: a high-pressure line connected with high-pressure accumulators and a low-pressure line connected directly to a tank. The CPR system is applied to vehicles and shows much reduction of energy consumption, according to 5) and 6). To utilize the advantage of the above hydraulic systems, a closed-loop hydrostatic transmission is proposed for braking energy regeneration with two hydraulic accumulators. The proposed system can be switched between two configurations: flow coupling configuration and pressure coupling configuration for the comparison of the effect of each configuration. The high pressure accumulator (HPA) plays an important role in the system, as discussed in 7). It functions as power source as well as energy storage to absorb the braking energy from the hydraulic pump/motor in braking time.

This paper is organized as follows: section 2 describes the proposed system and its operation; section 3 presents the mathematical model of the system; section 4 presents the simulation and analysis of the simulation results. Finally, conclusions are presented in the last section.

2. System description

The proposed system is a hydrostatic drive which transmits the power from the electric motor to the load, the flywheel FW. In comparison with a traditional HST, a directional control valve and two hydraulic accumulators (HPA, LPA) are added (Fig. 1). The high-pressure accumulator HPA functions as a storage system or a power supply, while the low-pressure accumulator LPA functions as a low-pressure, high-flow source for the hydraulic machine pump/motor during decelerating, and boosts the system during accelerating. The flywheel FW simulates external load. The secondary unit, the hydraulic pump/motor, could function as a hydraulic pump or a hydraulic motor depending on velocity, displacement and pressure difference between two ports of pump/motor.

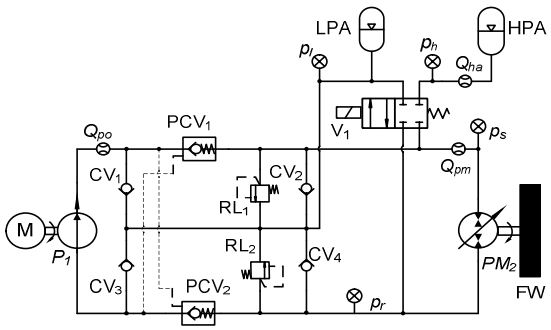

Fig. 1 Schematic diagram of the proposed system

The proposed system can operate in two distinguished configurations of hydraulic systems that are flow coupling configuration and pressure coupling configuration by controlling the directional control valve.

2.1 Flow coupling configuration

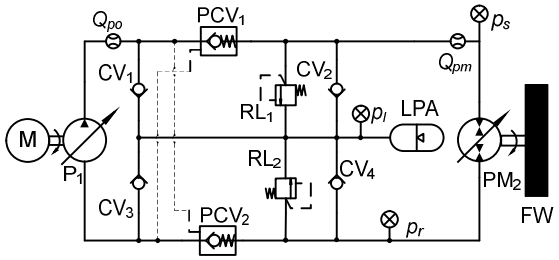

Fig. 2 Flow coupling configuration

When V_1 is OFF, the system operates as a closed-loop flow coupling hydrostatic transmission with over-velocity protection mechanisms, as in Fig. 2. The velocity of the flywheel FW is controlled by adjusting the displacement of pump P_1 while the displacement of hydraulic machine PM_2 is fixed. When the velocity of the flywheel is greater than reference velocity, the pressure in return line pr becomes high, while the pressure in the driving/supply line ps becomes low. Pilot check valve PCV_2 is then closed, and hydraulic energy in the form of high-pressure fluid is dissipated via the relief valve RL_2. This function is similar to that of a hydraulic brake, which reduces the velocity of the flywheel FW under the reference velocity. As the velocity of the flywheel in an HST is reduced, the kinetic energy of the flywheel is dissipated by braking. In the application of hydraulic vehicles, regenerative braking energy is substantial, so the recovery of regenerative energy may significantly reduce total energy consumption.

2.2 Pressure coupling configuration

When V_1 is ON, the system operates as a closed-loop pressure coupling hydrostatic transmission, as shown in Fig. 3. In this configuration, pump P_1 is ON/OFF controlled to compensate the pressure of HPA. The velocity of the flywheel is controlled directly by adjusting the displacement of the hydraulic machine PM_2.

In accelerating time, Fig. 3a, the driving line is connected to HPA while the return line is directly connected to LPA. The hydraulic machine PM_2 functions as a hydraulic motor that transfers the potential energy in the HPA into the kinetic energy of the flywheel. To accelerate the flywheel, the displacement of PM_2 is increased, and vice versa. In decelerating time, Fig. 3b, the hydraulic machine PM_2 functions as a hydraulic pump that pumps fluid from LPA to HPA. The kinetic energy of the flywheel is transformed to hydraulic energy stored in HPA. When the displacement of the hydraulic machine PM_2 increases, the impeded torque in the shaft of PM_2 also increases, so that the velocity of the flywheel decreases rapidly.

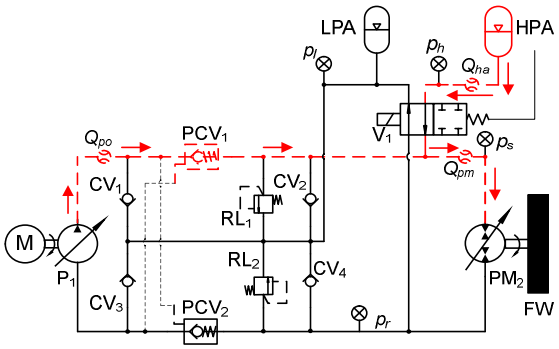

Fig. 3a Accelerating time in pressure coupling configuration

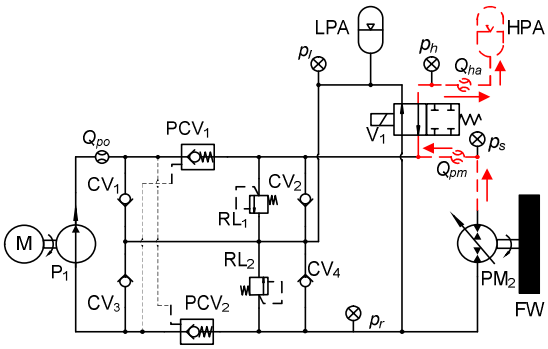

Fig. 3b Decelerating time in pressure coupling configuration

3. Mathematical Model

3.1 Analysis of efficiency

The ideal flow rates, volumetric and mechanical efficiencies of the piston hydraulic pump are expressed in Eq. (1), (2) and (3), respectively:

$$Q_i = \alpha \omega D_{\max} \tag{1}$$

$$\eta_{vP} = \frac{Q_i - Q_l}{Q_i} \tag{2}$$

$$\eta_{tP}=\frac{\alpha D_{\max}\Delta p}{\alpha D_{\max}\Delta p+T_l} \tag{3}$$

The actual output flow rate and input torque of the pump are expressed in Eq. (4) and (5), respectively:

$$Q_o=Q_i\eta_{pV} \tag{4}$$

$$T_i=\alpha\Delta pD_{\max}\eta_{tPM} \tag{5}$$

3.1.1 Motor mode

The volumetric efficiency, mechanical efficiency, actual flow rate and actual output torque of the piston hydraulic motor are expressed by Eq. (6) ~ (9), respectively.

$$\eta_{vM}=\frac{\alpha D_{\max}\omega}{\alpha D_{\max}\omega+Q_{loss}} \tag{6}$$

$$\eta_{tM}=\frac{\alpha D_{\max}\Delta p-T_{loss}}{\alpha D_{\max}\Delta p} \tag{7}$$

$$Q_m=\frac{Q_i}{\eta_{vM}} \tag{8}$$

$$T_m=\alpha\Delta pD_{\max}\eta_{tM} \tag{9}$$

3.1.2 Electro-hydraulic displacement control mechanism (DCM)

An electro-hydraulic mechanism is employed to regulate the angle of the swash plate for control the displacement of the hydraulic pump/motor. A full order model of the system is a fifth-order system with voltage input and the angle of the swash plate or the displacement of the pump/motor. However, in practical application of hydraulic systems, a reduced first-order is often used instead of the full order model[9)-11)]. In this study, a first-order model of the electro-hydraulic mechanism is used and expressed as:

$$u(t)=\frac{\tau}{K_{sv}}\dot{\alpha}+\frac{1}{K_{sv}}\alpha \tag{10}$$

3.2 Model of hydraulic accumulator

High pressure accumulator plays an important role in the switching closed loop HST. Its volume must be large enough to absorb the kinetic energy of vehicle during decelerating time but its size should be small because of the limit of space in vehicle. In such system, we employed bladder accumulator, which filled with nitrogen gas. According to 12), the nitrogen gas is assumed to compress and expand based on the adiabatic gas law:

$$pV^n=p_0V_0^n=p_{\max}V_{\min}^n \tag{11}$$

Then the fluid volume in the hydraulic accumulator HPA is derived as:

$$V_f=\begin{cases}0, if\ p_i\le p_0\\ V_0(1-\dfrac{p_0}{p_i})^{\frac{1}{n}}, else\end{cases} \tag{12}$$

The energy that can be absorbed by HPA is calculated as:

$$E=\frac{p_{\max}^{\frac{1}{n}}V_0}{n-1}\left[\lambda_p^{\frac{1}{n}}-\lambda_p\right] \tag{13}$$

where,

$$\lambda_p=\frac{p}{p_{\max}} \tag{14}$$

The optimal pre-charged pressure for maximum energy capacity of HPA is given by:

$$p_0=n^{n/(1-n)}p_{\max} \tag{15}$$

And the maximum energy stored in HPA is given by:

$$E_{\max}=p_{\max}V_0n^{n/(1-n)} \tag{16}$$

Then the volume of HPA is derived as:

$$V_0=\frac{E_{k,\max}}{p_{\max}n^{n/(1-n)}} \tag{17}$$

3.3 Model of connecting line

3.3.1 Flow coupling configuration

For simplicity, the pressure drop in the check valves is neglected, so the pressure before and after check valves is the same. Hydraulic accumulator LPA is large enough to make the pressure of accumulator constant. The dynamic response of the valves can be ignored when compared with that of the flywheel or system pressures. In the driving line, pressure p_s is expressed as:

$$\frac{dp_s}{dt}=\frac{\beta}{V_h}\left(Q_{po}+Q_b-Q_{r1}-Q_{mi}\right) \tag{18}$$

The return line is more sophisticated because the pressures at motor outlet pr and pump inlet ppi may be different depending on the state of the pilot check valve PCV_2. The pressure at the pump inlet port is expressed

as:

$$p_{pi}=\begin{cases} p_r & if\ p_s > p_{pcv2} \\ p_l & if\ p_s \le p_{pcv2} \end{cases} \quad (20)$$

Pressure p_r plays an important role in the system dynamics, and is expressed by:

$$\frac{dp_r}{dt}=\frac{\beta}{V_h}\left(Q_{mo}+Q_b-Q_{r2}-Q_{pi}\right) \quad (21)$$

$$Q_{r1,2}=\begin{cases} 0, & if\ \Delta p \le p_{rv} \\ K_{1,2}(\Delta p - p_{rv})\sqrt{\Delta p}, & if\ p_{rv} \le \Delta p \le p_{\max} \end{cases} \quad (22)$$

where

$$K_{1,2}=C_d\delta\frac{A_{r1,2}}{k}\sqrt{\frac{2}{\rho}} \quad (23)$$

The reference velocity of the flywheel at each instant is determined by the flow coupling principle expressed as:

$$\omega_{fl}=\frac{\omega_p D_p \eta_{vp}\eta_{vm}}{D_m} \quad (24)$$

3.3.2 Pressure coupling configuration

In the accelerating line pressure p_s is expressed as:

$$\frac{dp_s}{dt}=\frac{\beta}{V_h}\left(Q_{po}+Q_b-Q_{ha}-Q_{r1}-Q_{pm}\right) \quad (25)$$

where,

Qpm is expressed by Eq. (8) in accelerating time and Eq. by (4) in decelerating time.

$$Q_{ha}=\begin{cases} 0, & if\ p_i \le p_0 \\ \dfrac{d}{dt}\left[V_0\left(1-\dfrac{p_0}{p_i}\right)^{\frac{1}{k}}\right], & if\ p_i \le p_0 \end{cases} \quad (26)$$

$$\Delta p = p_s - p_r \quad (27)$$

where p_r is the returning line pressure, which is considered as the pressure in LPA in pressure coupling configuration.

3.3.3 Model of load

The dynamic equation of the flywheel FW is obtained by applying Newton's second law, as:

$$T_m = J\dot{\omega} + C\omega + T_{ex} \quad (28)$$

where T_{ex} is external load torque.

4. Simulation and Results

To analyze the response of the proposed system for vehicle applications, this system was applied to a 2000kg vehicle. Final reduction gear ratio is 3.55 and the radius of wheel is 0.28m. We employed 10-mode profile schedule, one of the typical driving schedules for vehicle testing, as a velocity reference to evaluate the performance of the proposed system. Setting parameters of the system model for simulations are shown in Table 1.

Table 1 Setting parameters of the system

Components	Capacity	Unit
Hydraulic machine		
displacement	[-55 55]	cc/rev
max pressure	250	bar
Flywheel		
inertial moment	4.5	kgm^2
viscous friction coef.	0.01	Nm/(RPM)
HPA		
volume	20	liter
gas-pre-charge	120	bar
max pressure	280	bar
LPA		
volume	50	liter
gas-pre-charge	2	bar
Electric motor		
power	25	HP
speed	1160	rpm

The simulations have been carried out in the following two cases: flow coupling configuration and pressure coupling configuration, using a PID controller for velocity control in both cases.

Firstly, simulation was carried out in flow coupling configuration. Fig. 4 shows the velocity response, error and displacement ratio of pump P_1, respectively in flow coupling configuration. This figure shows good performance in velocity response. The displacement α_1 of pump P_1 was regulated to achieve the reference velocity while the displacement α_2 of motor PM_2 was fixed at 0.9. The supply pressure and return pressure in flow coupling configuration are shown in Fig. 5. The supply pressure increases during the acceleration time and decreases during the deceleration time. In the contrary, return pressure increases during deceleration time or braking time and decreases during acceleration time. Fig. 6 shows the flow rate and fluid volume via hydraulic machine PM_2. In flow coupling configuration,

this flow rate proportional to the velocity of flywheel FW as shown in Eq.(24). The total fluid volume via PM_2 during 10 mode profile schedule is 61 liters. Fig. 7 indicates the supplied power and supplied energy by pump P_1. The supplied power varies to meet the demand of hydraulic machine PM_2 in accelerating and decelerating time. The sum energy supplied to 10 mode profile is 307.8kJ.

Secondly, simulation was carried out in pressure coupling configuration. Fig. 8 shows the velocity response, error and displacement ratio of hydraulic machine PM_2, respectively. This figure shows that the velocity response is better in comparison with it in flow coupling configuration. The displacement of motor PM_2 is regulated to reach the required torque and velocity as the system pressure changes while the displacement ratio pump P_1 was ON/OFF controlled to maintain the pressure in the high pressure accumulator HPA in a specified interval.

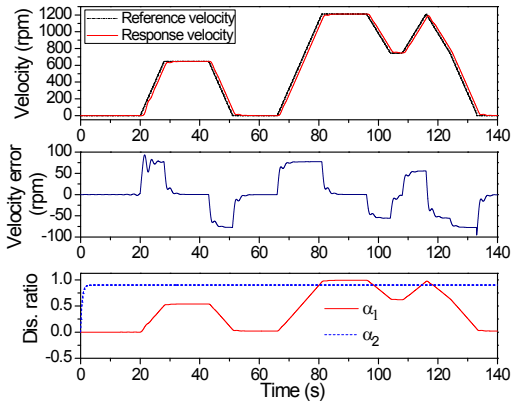

Fig. 4 Velocity, error and displacement ratio of pump P_1 in flow coupling configuration

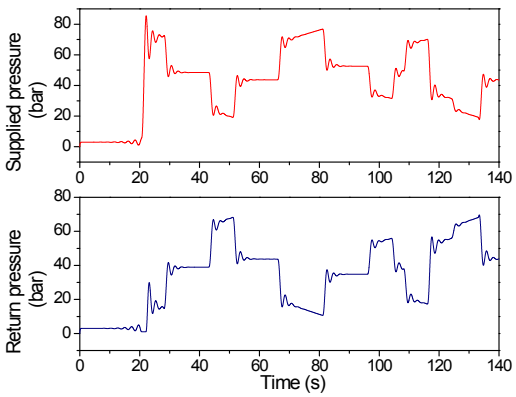

Fig. 5 Supplied pressure and return pressure in flow coupling configuration

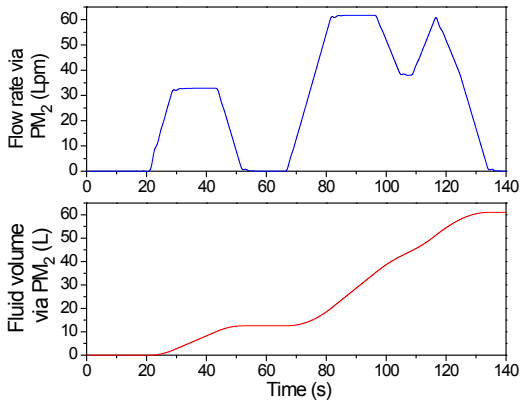

Fig. 6 Flow rate and fluid volume via hydraulic machine PM_2 in flow coupling configuration

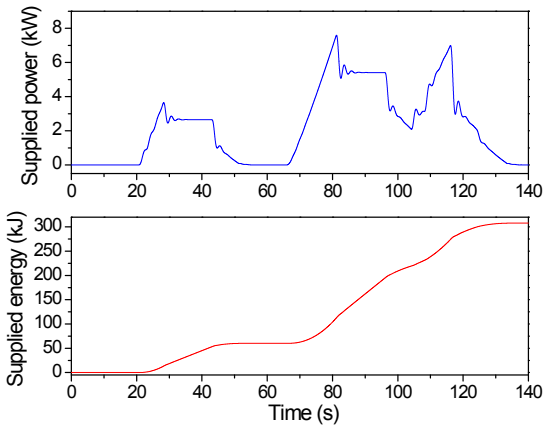

Fig. 7 Supplied power and energy in flow coupling configuration

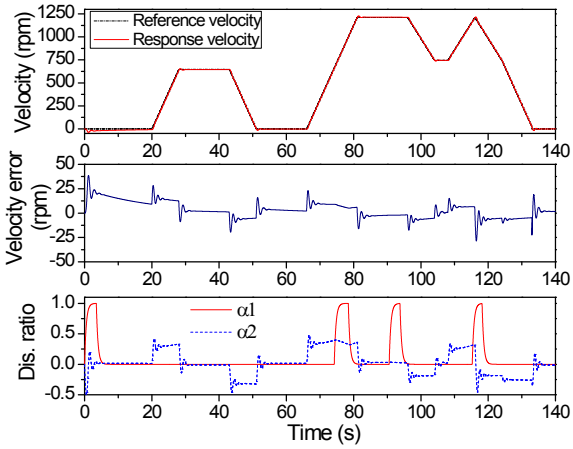

Fig. 8 Velocity, error and displacement ratio of PM_2 in pressure coupling configuration

The flow rate into the high accumulator is maximum until the pressure of HPA reaches to 160 bar and it is zero until the pressure decreases to 135bar (Fig. 9 ~ 10). The displacement of PM_2 is regulated to make driving or braking torque as in Eq. (9). Therefore, its

flow rate is positive in accelerating time and negative in decelerating time, and the sum of fluid via PM_2 is less than that of flow coupling configuration. The high pressure accumulator HPA stores energy from P_1, supplies hydraulic energy to hydraulic machine PM_2 in accelerating time and absorbs it from PM_2 in decelerating time. The flow rate of HPA increases as the flow rate of P_1 increases or the flow rate of PM_2 is negative, and it decreases as the flow rate of PM_2 increases. HPA power and energy are shown in Fig. 11. The supplied power and energy of pump P_1 are shown in Fig. 12. The supplied power is switched between zero and maximum value due to the displacement ratio of P_1. The sum energy supplied to 10 mode profile schedule in this configuration is 182.2kJ. It means that 125.6kJ or 40.8% supplied energy was reduced compared to that of flow coupling configuration.

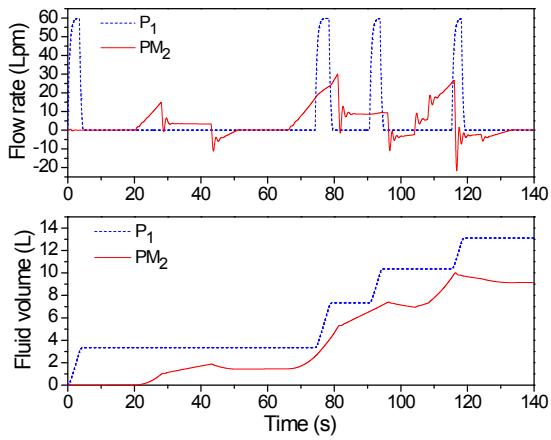

Fig. 9 Flow rate and fluid volume of P1 and PM2 in pressure coupling configuration

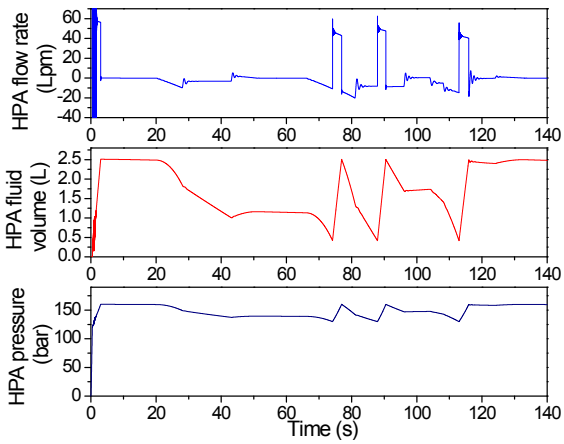

Fig. 10 Input flowrate, fluid volume and pressure of HPA in pressure coupling configuration

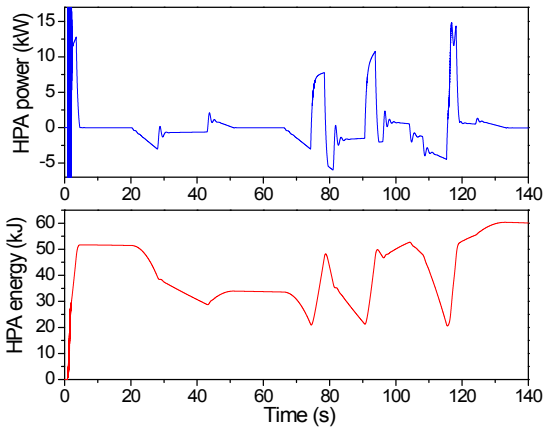

Fig. 11 Power and energy of HPA in pressure coupling configuration

Besides 10 mode profile schedule, simulation was also carried out in case of modified 10 mode profile and highway schedule in the same way.

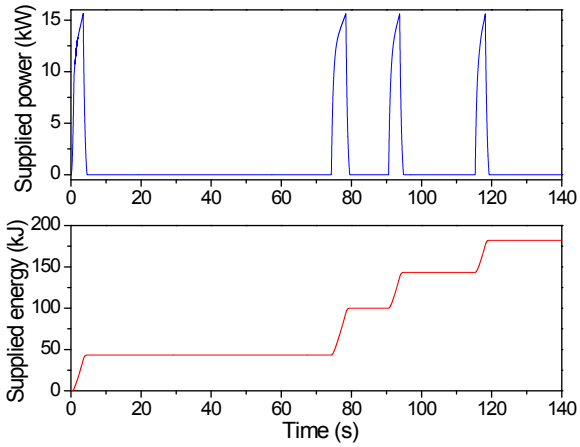

Fig. 12 Supply power and energy in pressure coupling configuration

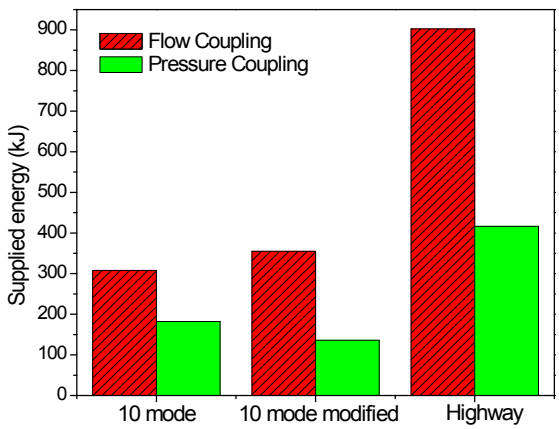

Fig. 13 Supply energy in 10 mode, 10 mode modified profile and highway schedule

The supplied energy for these three schedules is compared in Fig. 13. 61.7% and 53.8% of energy among the supply energy are reduced in 10 mode modified profile and highway schedule, respectively. This result means that the proposed pressure coupling hydrostatic transmission is superior in energy consumption reduction in three road driving schedules.

5. Conclusions

A closed-loop hydrostatic transmission with two different configurations (flow coupling and pressure coupling) was proposed and investigated in this research. All hydraulic components were mathematically modeled based on parameters of a real hydraulic system.

This simulation results proved that the pressure coupled hydrostatic transmission had better energy efficiency compared to that of flow coupling one and from the simulation results, 40.8%, 61.7% and 53.8% supplied energy was reduced in 10 mode, modified 10 mode and highway profile, respectively when pressure coupling configuration was adopted.

References

1) M. Martelli *et al.*, “Hydrostatic Transmission with a Traction Control,” 22nd ISARC, 2005.
2) H. Shimoyama *et al.*, “Study on Hybrid Vehicle Using Constant Pressure Hydraulic System with Flywheel for Energy Storage”, SAE 2004-01-3064, 2004.
3) T. H. Ho *et al.*, “A Study on Energy Saving Potential of Hydraulic Control System Using Switching Type Closed Loop Constant Pressure System,” Proc. of the Int. Conf. JFPS, Vol. 2, pp. 317-322, 2008.
4) H. Yang *et al.*, “New investigation in energy regeneration of hydraulic elevators,” IEEE/ASME trans. on Mech., Vol. 12, No. 5, pp. 519~526, 2007.
5) R. Johri *et al.*, “Low-cost pathway to ultra efficiency car: Series hydraulic hybrid system with optimized supervisory control,” SAE, Vol. 2, No. 2, pp. 505~520, 2010.
6) P. Matheson *et al.*, “Modeling and simulation of a fuzzy logic controller for a hydraulic hybrid powertrain for use in heavy commercial vehicles,” SAE 2003-01-3275, 2003.
7) Y. M. Jen *et al.*, “Influence of an accumulator on the performance of a hydrostatic drive with control of the secondary unit,” IMechE, Vol. 207, No. 13, pp. 173~184, 1993.
8) T.H. Ho *et al.*, “Modeling and Simulation of a Hydrostatic Transmission System with Energy Recuperation Using a Hydraulic Accumulator”, JMST, Vol. 24, No. 5, pp. 1163~1175, 2010.
9) H. Berg *et al.*, “Design and testing of a robust linear controller for secondary controlled hydraulic drive”, IMechE, Vol. 213, pp. 375~386, 1999.
10) C.S. Kim *et al.*, “Speed control of an over-centered variable displacement hydraulic motor with a load torque observer”, Control Engineer Practice, Vol. 4, pp. 1563~1570, 1996.
11) C.S. Kim *et al.*, “Robust Speed Control of a Variable-Displacement Hydraulic Motor Considering Saturation Nonlinearity,” ASME, Vol. 122, pp. 196~201, 2000.
12) B. Surampudi *et al.*, “Design and Control Considerations for a Serial Heavy Duty Hybrid Hydraulic Vehicle”, SAE 2009-01-2717, 2009.
13) M.G. Rabie, “Fluid Power Engineering”, McGraw-Hill, 2009.
14) J. I. Yoon *et al.*, “Development of Hybrid Excavator for Regeneration of Boom Potential Energy”, Trans. of KFPS, Vol.6, No. 4, pp.1-8, 2009.
15) S.W. Choi and J. Y. Hur, “Dynamic Analysis on the Tail Gate System for Vehicle with the Energy Regenerative Brake of Hydraulic Driven Systems,” Trans. of KFPS, Vol.7, No. 2, pp.19~26, 2010.
16) S. H. Cho, “Path Control with Energy-Saving Load-Sensing for a Cylinder-Load System Using Speed-Controlled Fixed Displacement Pump,” Trans. of KFPS, Vol.6, No. 3, pp.16~22, 2009.